

LHC Electroweak Working Group
Precision Subgroup Meeting – 9 July 2020

F Hautmann

Nonperturbative contributions to
vector boson transverse momentum spectra
in hadronic collisions

- based on Phys. Lett. B 806 (2020) 135478 [arXiv:2002.12810]

collaboration with I Scimemi and A Vladimirov

DRELL-YAN (DY) PRODUCTION AT $q_T \ll Q$

- It was realized long ago that DY vector-boson transverse momentum spectra are affected for $q_T \ll Q$ by large dynamical effects beyond collinear factorization:
 - perturbative logarithmically-enhanced corrections in $\alpha_s^n \ln^m(Q/q_T)$
 - nonperturbative contributions besides PDFs due to
 - i) intrinsic k_T distribution of initial states and
 - ii) nonperturbative components of Sudakov form factors.

*[Parisi-Petronzio, NPB 154 (1979) 427
Curci-Greco-Srivastava, NPB 159 (1979) 451
Dokshitzer-Diakonov-Troian, Phys Rep 58 (1980) 269
Collins-Soper, NPB 193 (1981) 381]*

CSS formalism and TMDs

- The summation of DY logarithmically-enhanced corrections can be accomplished by methods based on the CSS formalism

[Collins-Soper-Sterman, NPB 250 (1985) 199]

- Nonperturbative effects besides PDFs can be included in the formalism of transverse momentum dependent (TMD) distribution functions:

- intrinsic k_T distributions enter as boundary conditions to mass evolution equations for TMDs
- nonperturbative Sudakov effects enter through kernel of rapidity evolution equations for TMDs

[Collins, Foundations of perturbative QCD, CUP 2011]

PHENOMENOLOGICAL STUDIES OF NONPERTURBATIVE TMD EFFECTS

- Pioneering studies by Resbos

[Ladinsky-Yuan, PRD 50 (1994) R4239

Landry et al, PRD 63 (2001) 013004

Landry et al, PRD 67 (2003) 073016

Konychev-Nadolsky, PLB633 (2006) 710]

- Recent studies by Artemide and NangaParbat

[Scimemi-Vladimirov, arXiv:1912.06532;

Bacchetta et al, arXiv:1912.07550]

- The study *Phys. Lett. B 806 (2020) 135478* presented in this talk

uses Artemide. It focuses on

- the interplay of two nonperturbative effects – Sudakov and intrinsic kT
 - the behavior of the rapidity evolution kernel at large distances
 - the role of precision LHC measurements for TMD determinations

Basic Elements of the Approach

- Low- q_T factorization/evolution

We start from the TMD factorization formula for the differential cross section for DY lepton pair production $h_1 + h_2 \rightarrow Z/\gamma^*(\rightarrow ll') + X$ at low $q_T \ll Q$ [13]

$$\frac{d\sigma}{dQ^2 dy dq_T^2} = \sigma_0 \sum_{f_1, f_2} H_{f_1 f_2}(Q, \mu) \int \frac{d^2 \mathbf{b}}{4\pi} e^{i\mathbf{b} \cdot \mathbf{q}_T} F_{f_1 \leftarrow h_1}(x_1, \mathbf{b}; \mu, \zeta_1) F_{f_2 \leftarrow h_2}(x_2, \mathbf{b}; \mu, \zeta_2) + \mathcal{O}(q_T/Q) + \mathcal{O}(\Lambda_{\text{QCD}}/Q), \quad (1)$$

where Q^2 , q_T and y are the invariant mass, transverse momentum and rapidity of the lepton pair, and the TMD distributions $F_{f \leftarrow h}$ fulfill evolution equations in rapidity

$$\frac{\partial \ln F_{f \leftarrow h}}{\partial \ln \zeta} = -\mathcal{D}^f(\mu, \mathbf{b}) \quad (2)$$

and in mass

$$\frac{\partial \ln F_{f \leftarrow h}}{\partial \ln \mu} = \gamma_F(\alpha_s(\mu), \zeta/\mu^2), \quad \frac{\partial \mathcal{D}^f(\mu, \mathbf{b})}{\partial \ln \mu} = \frac{1}{2} \Gamma_{\text{cusp}}(\alpha_s(\mu)) . \quad (3)$$

- Small- \mathbf{b} expansion

We further perform the small- \mathbf{b} operator product expansion of the TMD $F_{f \leftarrow h}$ as follows,

$$F_{f \rightarrow h}(x, \mathbf{b}) = f_{\text{NP}}(x, \mathbf{b}) \sum_{f'} \int_x^1 \frac{dy}{y} C_{f \leftarrow f'} \left(\frac{x}{y}, \ln(\mathbf{b}^2 \mu^2) \right) f_{f' \leftarrow h}(y, \mu), \quad (4)$$

where $f_{f' \leftarrow h}$ are the PDFs, $C_{f \leftarrow f'}$ are the matching Wilson coefficients, and f_{NP} are functions¹ to be fitted to data.

Perturbative summation

- The summation of logarithmically-enhanced corrections at low q_T is achieved by computing perturbatively the functions H , C , γ and Γ as series expansions in powers of α_s

| H | $C_{f \leftarrow f'}$ | Γ_{cusp} | γ_F | α_s running | PDF evolution |
|--------------|-----------------------|------------------------|--------------|--------------------|---------------|
| α_s^2 | α_s^2 | α_s^3 | α_s^3 | NNLO | |

Table 1: Summary of perturbative orders used for each part of the DY cross section.

(NNLL logarithmic accuracy)

- Scale setting for double-scale evolution in $(zeta, \mu)$ by “zeta prescription”.

Nonperturbative contributions I: rapidity evolution kernel

- Write D using b^* prescription as

$$\mathcal{D}^f(\mu, \mathbf{b}) = \mathcal{D}_{\text{res}}^f(\mu, b^*(\mathbf{b})) + g(\mathbf{b}), \quad \text{where} \quad b^*(\mathbf{b}) = |\mathbf{b}| \sqrt{\frac{B_{\text{NP}}^2}{b^2 + B_{\text{NP}}^2}}$$

- Nonperturbative component of rapidity evolution kernel modeled and fitted to data:

$$g(\mathbf{b}) = g_K \mathbf{b}^2,$$

quadratic behavior
(traditionally used in TMD fits since Resbos)

$$g(\mathbf{b}) = c_0 |\mathbf{b}| b^*(\mathbf{b}),$$

linear rise at large b

$$g(\mathbf{b}) = g_K^* \mathbf{b}^{*2},$$

quadratic at small b , constant at large b
(similar spirit to parton saturation in s-channel
picture [Soper & H, PRD 75 (2007) 074020])
 $d D / d \ln b = 0$ for large b

- Zeta prescription scale setting [A. Vladimirov, arXiv:1907.10356]

$$\zeta_{\text{NP}}(\mu, b) = \zeta_{\text{pert}}(\mu, b) e^{-b^2/B_{\text{NP}}^2} + \zeta_{\text{exact}}(\mu, b) (1 - e^{-b^2/B_{\text{NP}}^2}).$$

Nonperturbative contributions II: intrinsic transverse momentum distribution

- Intrinsic kT modeled by Gaussian/exponential parameterizations and fitted to data:

$$f_{\text{NP}}(x, \mathbf{b}) = \exp\left(-\frac{(\lambda_1(1-x) + \lambda_2x + \lambda_3x(1-x))\mathbf{b}^2}{\sqrt{1 + \lambda_4x^{15}\mathbf{b}^2}}\right)$$

- Dependence on flavor and on kinematic convolution variable not included yet

TMD Global Fit

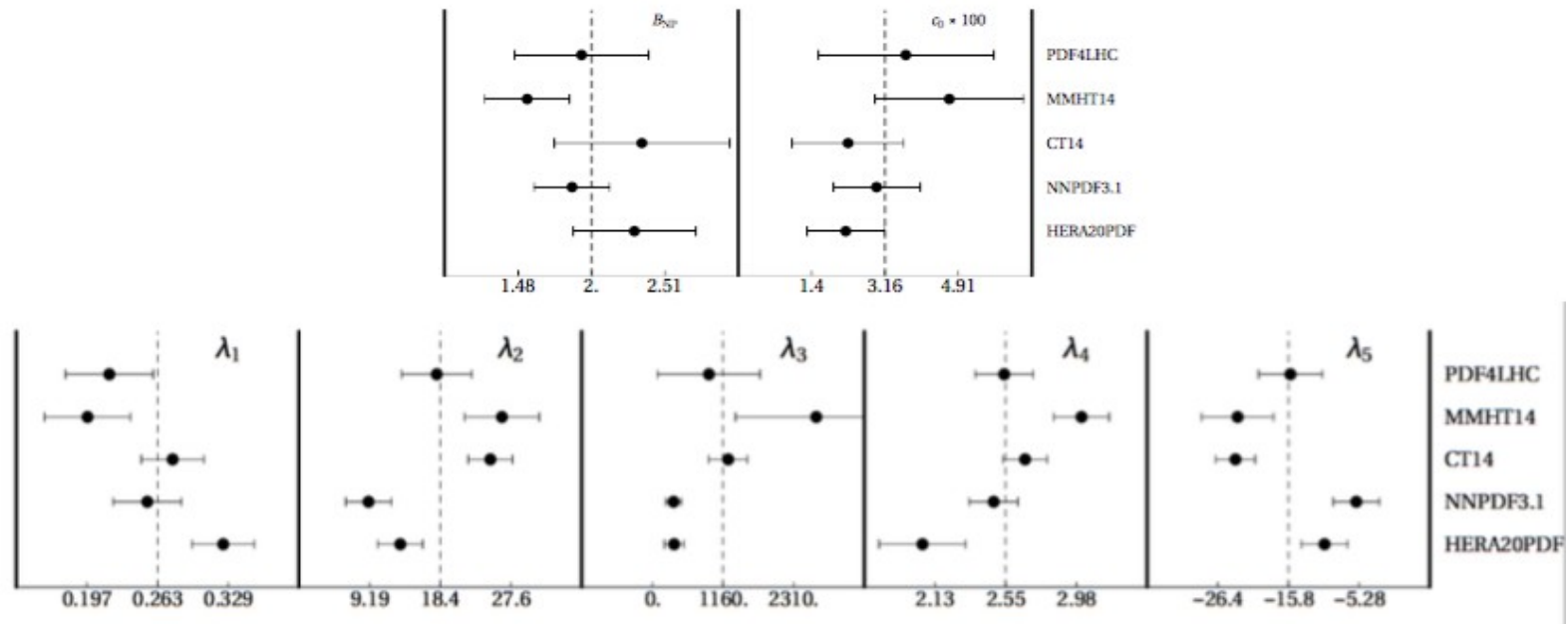


Figure 1: Results of the TMD global fit to DY measurements from LHC and lower-energy experiments.

| PDF | $\chi^2/\text{d.o.f.}$ |
|-----------------|------------------------|
| NNPDF3.1 [63] | 1.14 |
| HERAPDF2.0 [64] | 0.97 |
| CT14 [65] | 1.59 |
| MMHT14[66] | 1.34 |
| PDF4LHC [67] | 1.53 |

Table 2: PDF sets and $\chi^2/\text{d.o.f.}$ results in a TMD global fit to DY measurements.

lambda parameters vary more significantly among different PDF sets than B and c parameters

Correlation of TMD parameters for different PDF sets

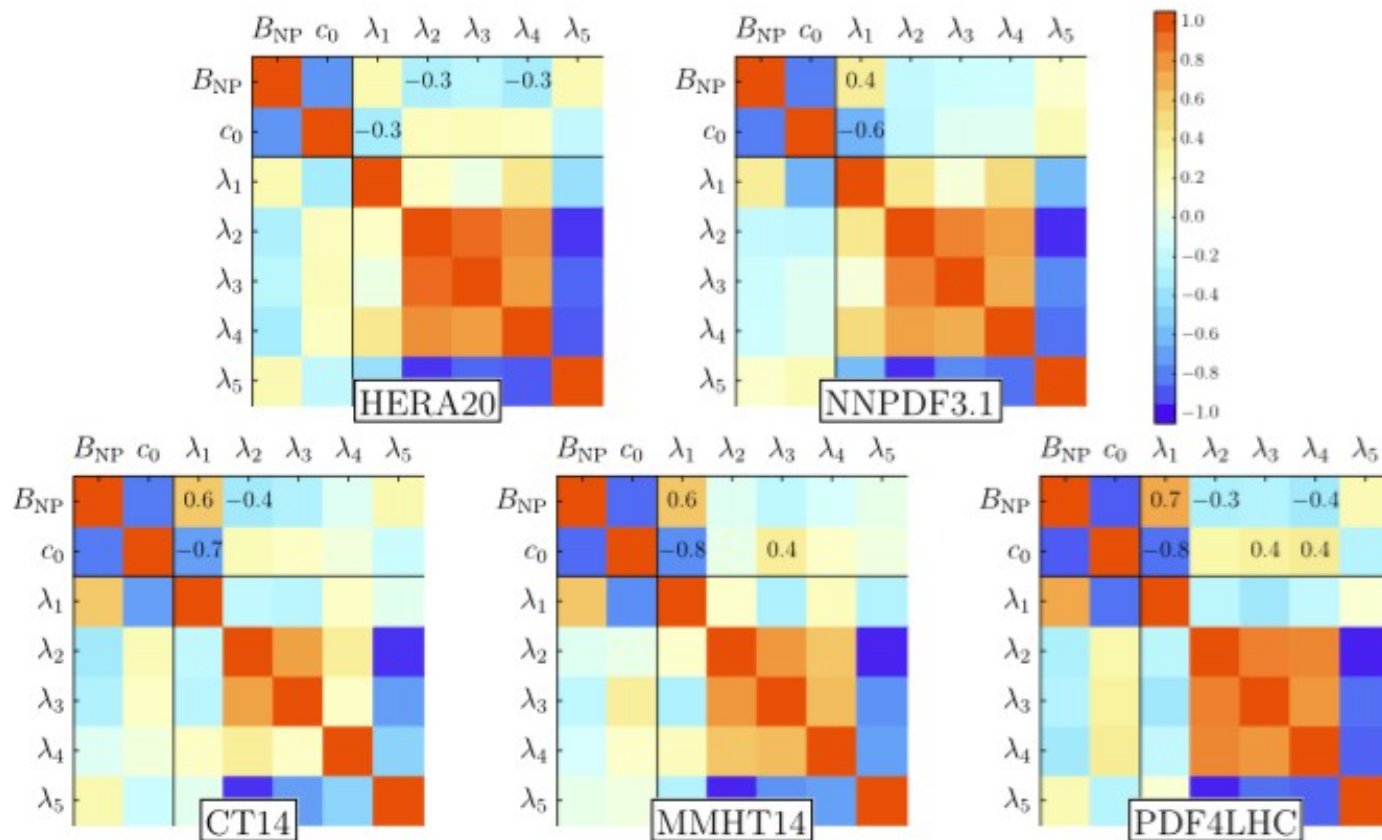


Fig. 3. Correlations of TMD fit parameters. In the axes $1 = B_{NP}$, $2 = c_0$, $(3, 4, 5, 6, 7) = \lambda_{1,2,3,4,5}$. Low correlation is represented by light colors, high correlation by dark colors. (The diagonal entries are trivial.)

- Correlations vary with PDF sets

The cut $q_T / Q < \delta$

- We vary the cut δ on the data set
- The δ dependence is mild between 0.1 and 0.25 both for the χ^2 and for the parameter values

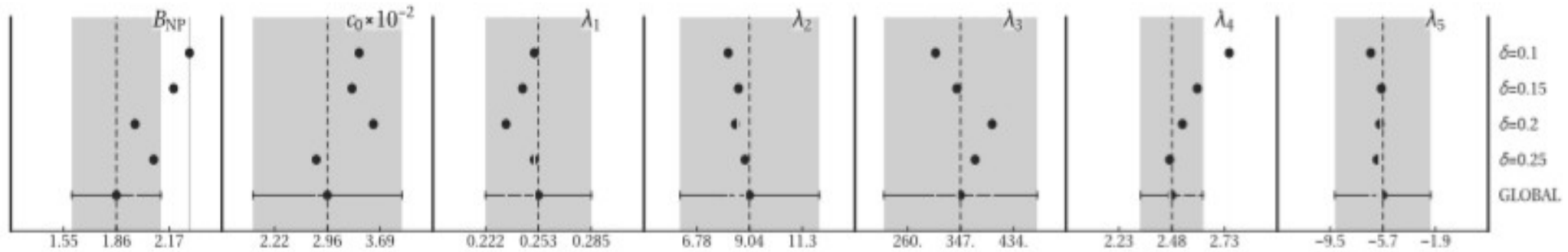


Fig. 2. Dependence of the values of the fitted TMD parameters on the δ cut (NNPDF3.1 PDF set).

- Matching with high q_T region is not included yet

The role of precision LHC measurements

2-parameter fits (cases 1, 3, 5): no intrinsic kT

3-parameter fits (cases 2, 4, 6): both nonperturbative Sudakov and intrinsic kT

| Case | B_{NP} | g_K | λ_1 ($f_{NP} = \exp -\lambda_1 b^2$) | χ^2/dof | $\chi^2/dof(norm.)$ |
|------|-----------------|-------------------|--|--------------|---------------------|
| 1 | 5.5 (max) | 0.116 ± 0.002 | 10^{-3} (fixed) | 3.29 | 3.04 |
| 2 | 2.2 ± 0.4 | 0.032 ± 0.006 | 0.29 ± 0.02 | 1.50 | 1.28 |
| Case | B_{NP} | c_0 | λ_1 | χ^2/dof | $\chi^2/dof(norm.)$ |
| 3 | 1. (min) | 0.016 ± 0.001 | 10^{-3} (fixed) | 2.21 | 1.99 |
| 4 | 3.0 ± 1.5 | 0.04 ± 0.02 | 0.27 ± 0.04 | 1.61 | 1.36 |
| Case | B_{NP} | g_K^* | λ_1 | χ^2/dof | $\chi^2/dof(norm.)$ |
| 5 | 1.34 ± 0.01 | 0.16 ± 0.01 | 10^{-3} (fixed) | 1.70 | 1.52 |
| 6 | 2.43 ± 0.66 | 0.05 ± 0.02 | 0.24 ± 0.04 | 1.49 | 1.28 |

Table 3: Results of 3-parameter and 2-parameter fits. The PDF set used is NNPDF3.1 [63].

- 3-parameter cases similar to global fit results
- Case 6: saturating behavior $dD/d \ln b = 0$

$$R_\sigma = 2 \frac{d\sigma^{\text{test}} - d\sigma^{\text{TMD}}}{d\sigma^{\text{test}} + d\sigma^{\text{TMD}}}, \quad (12)$$

- 2-parameter fits lead to higher chi2 values and different fitted parameters for rapidity kernel.
- I.e., intrinsic kT effects may be reabsorbed by changes in D.

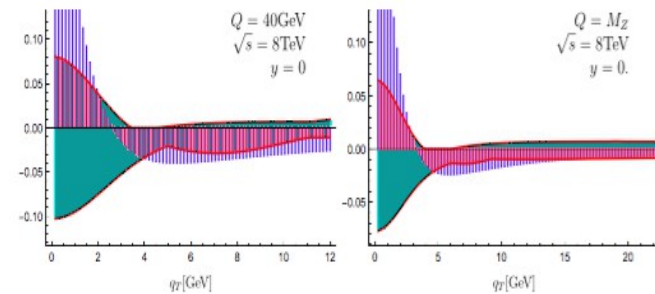
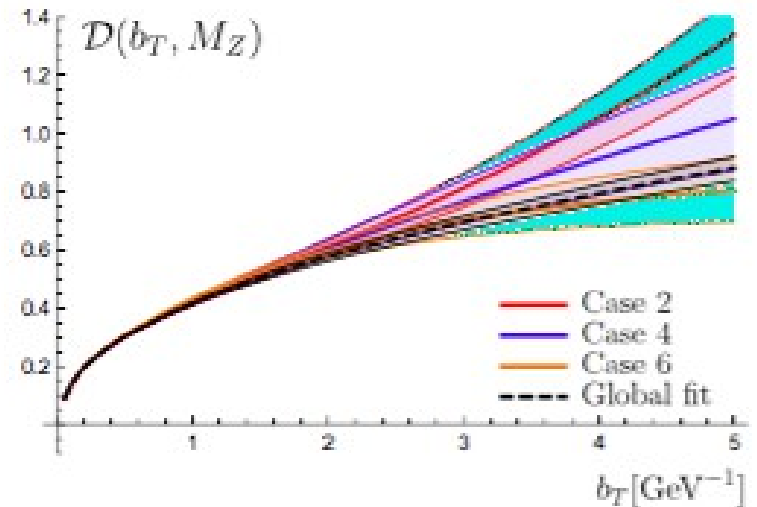
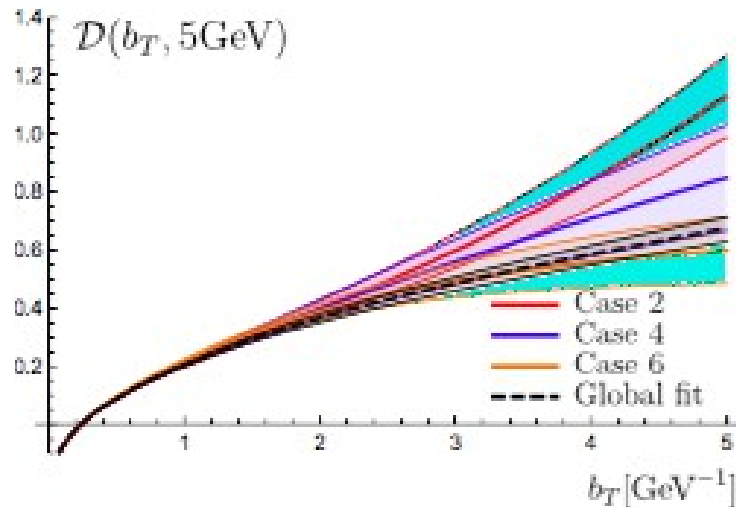
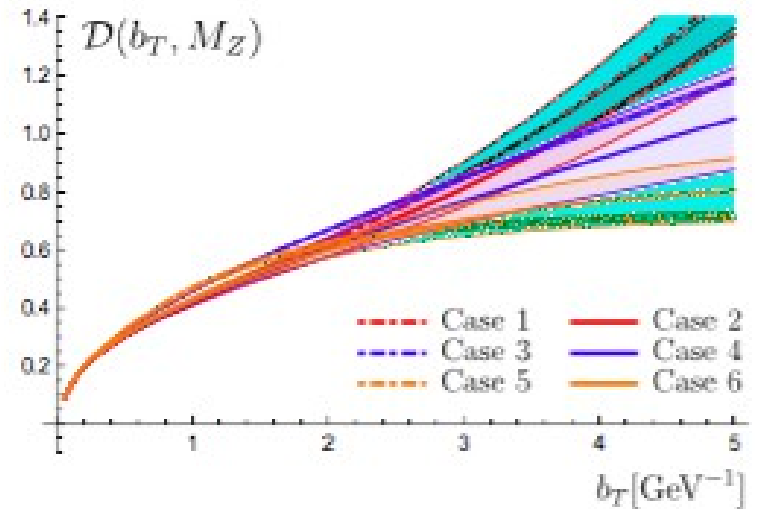
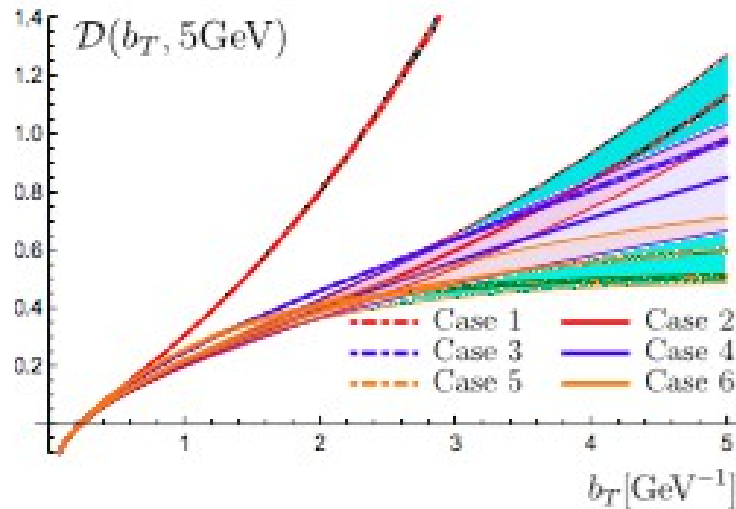


Figure 4: Sensitivity to nonperturbative physics in LHC DY measurements: the transverse momentum dependence of the ratio in Eq. (12), for central rapidity and different values of the lepton-pair invariant mass. The solid band is obtained from perturbative scale variation.

Given the reduction of perturbative uncertainties due to high logarithmic accuracy, residual uncertainty from nonperturbative TMD effects is non-negligible at low q_T and increasing with decreasing masses.

RAPIDITY EVOLUTION KERNEL

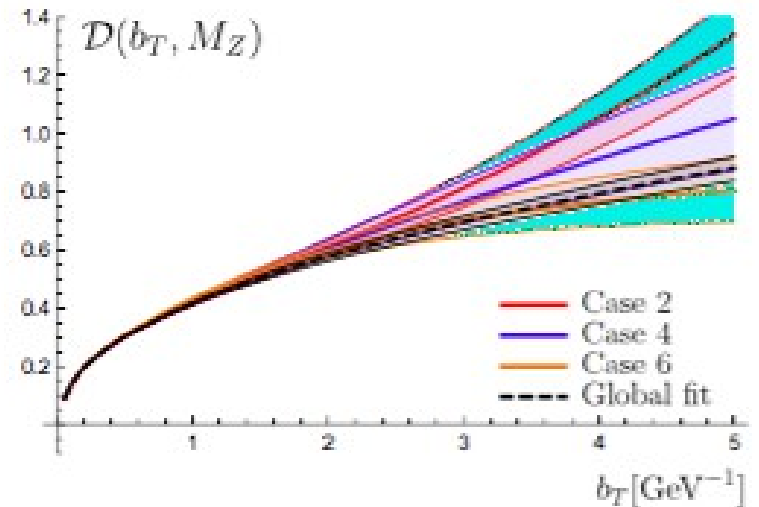
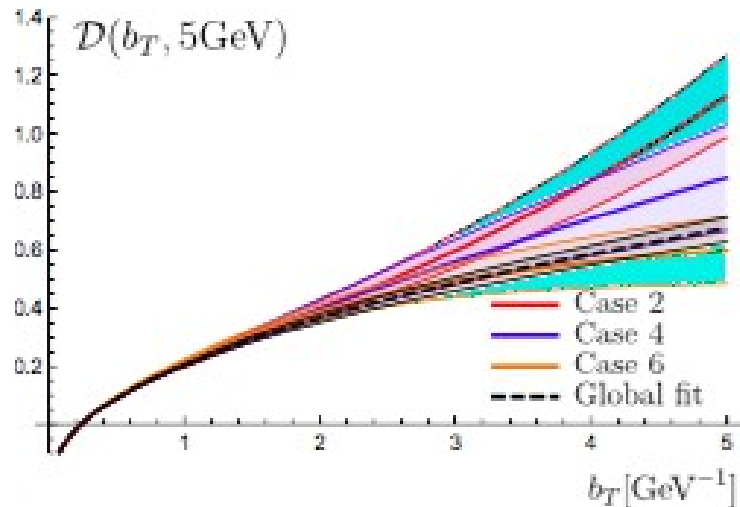
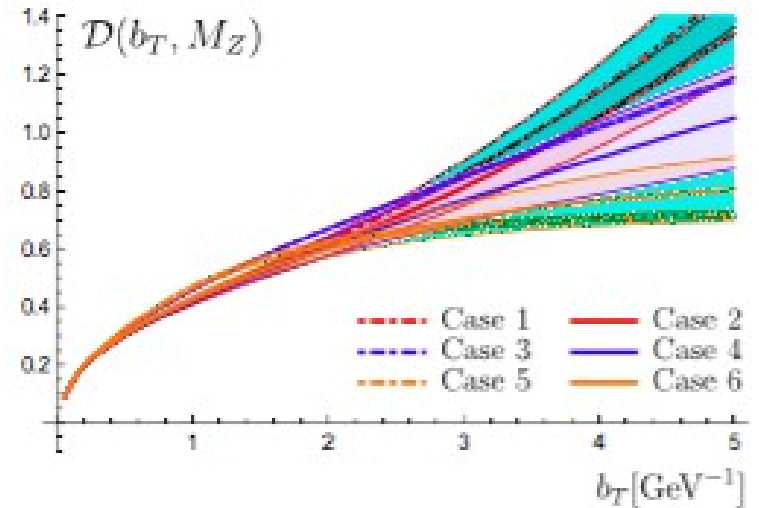
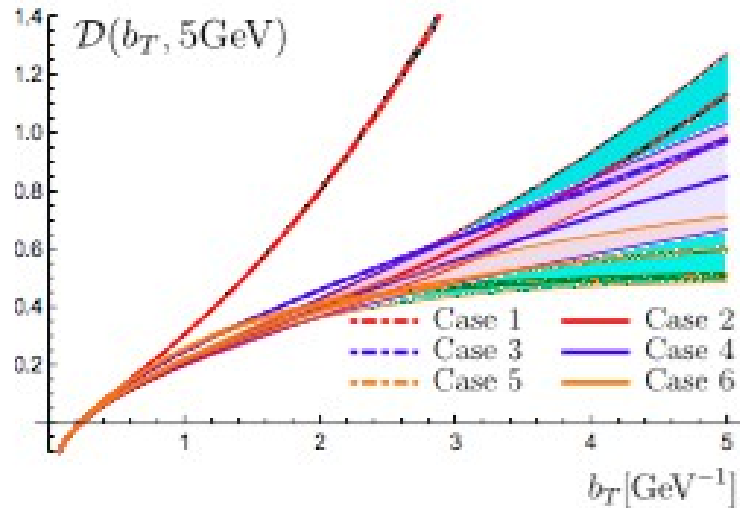
- Red curves: quadratic D; yellow curves: saturating D; blue curves: linear D.
- For each color, difference between solid and dashed curves measures correlations between Sudakov and intrinsic kT effects.



Quadratic model implies more pronounced dependence on intrinsic kT than the others (showing up especially for low masses)

RAPIDITY EVOLUTION KERNEL

- Limited sensitivity of current LHC measurements to long-distance region results into sizeable uncertainty bands at large b
- Higher sensitivity from low- q_T measurements with fine binning in q_T at low masses



- Global fit result in lower panels illustrates role of low-energy data: performed with linear model – but lower than blue curve and closer to yellow (saturating) curve

Conclusions

- Used low- q_T TMD factorization to investigate sensitivity of LHC and low-energy DY measurements to nonperturbative f and D , and correlations with collinear PDFs.
- Although strongest nonperturbative sensitivity is from low energy, neglecting any intrinsic k_T at the LHC worsens quality of fits and causes potential bias in determination of rapidity evolution kernel
- Residual uncertainty from nonperturbative TMD effects non-negligible in lowest q_T bins (increasing with decreasing masses)
- Results on large- b behavior of rapidity evolution kernel complementary to lattice studies – e.g. linear vs. saturating behavior
- Matching with high q_T region yet to be included